esa climate change initiative

European Space Agency

Climate-Space X-ECV

Karakoram Anomaly

ECV Inventory Document (EID)

Prepared by:	X-ECV consortium
Contract:	4000145271/24/I-LR
Name:	X-ECV_KA_D2.1_EID
Version:	0.2
Date:	30.03.2025

Contact:
Frank Paul
Department of Geography
University of Zurich
frank.paul@geo.uzh.ch

Technical Officer:
Anna Maria Trofaier
ESA Climate Office

University of Zurich[UZH] · UNIVERSITY OF OSLO · ETH zürich · enveo · University of BRISTOL · DWD · CLS COLLECTE LOCALISATION SATELLITES · GAMMA REMOTE SENSING

Document status sheet

Version	Date	Changes	Approval
0.1	22.01.2025	Initial draft	
0.2	30.03.2025	Consortium input included	

The work described in this document was done under ESA contract 4000145271/24/I-LR (Climate-Space X-ECV: Karakoram Anomaly). Responsibility for the contents resides with the authors who prepared it.

Author team:
Frank Paul (GIUZ), Thomas Nagler, Gabriele Schwaizer, Nico Mölg (ENVEO), Andreas Kääb, Désirée Treichler (GUIO), Lander van Tricht, Matthias Huss (ETHZ), Tazio Strozzi (Gamma), Fabien Maussion (UB), Rainer Hollmann (DWD), Christophe Fatras (CLS)

Glaciers_cci+ Technical Officer at ESA:
Anna Maria Trofaier

Related documents

Acronym	Acronym	Name	Version	Date
[RD1]	F4PR	Deliverable 2.2: Fit 4 Purpose Report	0.1	In prep.

Table of Contents

1. Purpose

This is the ECV inventory document (EID) of the X-ECV Karakoram Anomaly project. It is listing characteristics of the datasets to be used for the project along with their URLs. For a better description in a table, the datasets are sorted into three categories (glacier, climate and auxiliary data). All datasets are made internally available for further processing.

2. Introduction

To model glacier mass balance, we need several input datasets. Some are related to glacier extents and characteristics, others to climate and auxiliary datasets. We have grouped them into these three categories and list here the original datasets and their sources as used as the main input for the project. Several of these datasets will be modified in a second step to get them fit for purpose, i.e. suitable for application in the mass balance model and for further analysis. These adjustments will be described in a further document, the 'Fit for Purpose Report' or F4PR [RD1]. In cases where several input datasets are available for a specific application (e.g. reanalysis datasets) and the one to be selected is yet unclear, several of them are listed here.

3. Glacier data

3.1 Overview

Several of the glacier-related datasets have been derived from satellite data. These can be sorted into glacier outlines, surge inventories, debris cover (extent and thickness), geodetic mass balance, snow cover and flow velocities. The datasets differ in format (vector, raster), temporal coverage (single year, time series) and spatial coverage (Karakoram, HMA, global) and thus in file size. Table 1 provides the sources to the files without considering that we will extract spatial and/or temporal subsets for our applications and analysis in a second step.

Table 1: Glacier-related datasets, mostly derived from EO data. Datasets G1 & G2 are in vector, all others are in raster format. The URL for all datasets is listed below the table.

ID	Type	Region	Epoch	Description	Reference	URL
G1	Glacier outlines	RGI 14	1999-2005	Outlines & divides by Sakai 2019	RGI 7.0	1
G2	Surge inventory	Karakoram	historic & 1990-2015	Surge info from the literature & analysis of Landsat time-series	Bhambri et al. 2017	2
G3a	Debris extent	global	2013-2017	Landsat 8 & Sentinel-2 (based on RGI 6.0 outlines – mapped clean ice)	Scherler et al. 2018	3
G3b	Debris extent	global		updated RGI 6.0 extents (if >1 km^2), 255 hand-selected Landsat images	Herreid & P. 2020	4
G3c	Debris extent	Karakoram	1990-2022	Part of the surface classification. (G6a)	Glaciers_cci	5
G4a	Debris thickness	Global	2013-2018	Inversion from dh/dt & flux divergence + Landsat 8 temperature, see webpage	Rounce et al. 2021	6
G4b	Debris thickness	Baltoro	2004	Field data and ASTER-derived map	Mihalcea et al. 2008	7
G5a	Mass balance	global	2000-2019 (5 yr steps)	Time-series processing of ASTER data, global dataset	Hugonnet et al. 2021	8
G5b	Mass balance	Karakoram	2000-2010-2010-2016	From ASTER & SPOT DEMs, csv file for 403 glaciers, dh/dt grid upon request	Berthier & Brun 2019	9
G5c	Mass balance	HMA	2000-2018	From World View & ASTER DEMs	Shean et al. 2020	10
G6a	Snow cover	Karakoram	1990-2022	Time series from Landsat & Sentinel-2	Glaciers_cci	11
G6b	Snow cover	Hunza basin	2013	For comparison, data from author upon request	Racoviteanu et al. 2019	12
G6c	Snow cover	HMA	2000-2022	Daily seasonal snow cover outside mountain regions from MODIS for long term trend	Schwaizer et al. 2024	13
G7a	Velocity	global	2017/18	Composite from Sentinel-1/2, & Landsat 8 at 50 m res.	Millan et al. 2022	14
G7b	Velocity	HMA	1985-2017	Annual maps from Landsat data (240 m res.), available through ITS-LIVE	Dehecq et al. 2019	15
G7c	Velocity	Karakoram	2007-2011	Composite from SAR data	Rankl et al. 2014	16
G7d	Velocity	Karakoram	2007-2011	Summer & winter maps ALOS PALSAR FBD / FBS data at 100 m res.	Glaciers_cci	17
G7e	Velocity	Global	1985-present	Annual maps from Landsat, Sentinel-1/2 (240 m res.), incl. instant global data access to flow speed time-series	Gardner et al. 2019	18
G8a	Ablation data	Baltoro	July 2004	Ablation rates over 11 d for 23 points, request coordinates & elevation	Mihalcea et al. 2008	19
G8b	Accumulation	Urduk Glacier	2006	240/330/225/160 mm we at 5300 m per season, request coordinates	Mayer et al. 2014	20

Dataset URL:
1: https://nsidc.org/data/nsidc-0770/versions/7
2: https://doi.org/10.1038/s41598-017-15473-8 (Suppl. Table S1 was converted to a shapefile)
3: https://dataservices.gfz-potsdam.de/panmetaworks/showshort.php?id=escidoc:3473902
4: https://zenodo.org/records/3866466
5: Internal ftp-server
6: https://nsidc.org/data/hma_dte/versions/1
7: https://doi.org/10.3189/172756406781812104 (data in publication, grid: ask Milano)
8: https://doi. org/10.6096/13
9: https://doi.org/10.1017/jog.2019.32
10: https://zenodo.org/ record/3600624, DEM data: https://nsidc. org/data/highmountainasia
11: Internal-ftp server
12: https://doi.org/10.3389/feart.2019.00220
13: https://catalogue.ceda.ac.uk/uuid/80567d38de3f4b038ee6e6e53ed1af8a/
14: https://doi.org/10.6096/1007
15: https://its-live.jpl.nasa.gov
16: https://www.fau.eu/2021/08/news/research/tracking-glacial-velocity-online
17: https://glaciers-cci.enveo.at
18: https://its-live.jpl.nasa.gov
19: from paper
20: from paper

3.2 Short descriptions

14: A comprehensive high-resolution mapping of ice motion for 98% of the world's total glacier area during the period 2017–2018, presented by Millan et al. (2022), was used to make an improved estimate of the bed of the world's glaciers to generate an estimate of global ice volume that reconciles ice thickness distribution with glacier dynamics and surface topography.

15: Observations of changes in ice flow for all glaciers in High Mountain Asia over the period 2000–2017, based on one million pairs of optical satellite images, were compiled by Dehecq et al. (2019).

16: Rankl et al. (2014) compiled velocity measurements from SAR sensors in the period 2007–2011 , giving priority in subsequent order to the highest resolution, the best SNR, and closest acquisition date.

17: Flow velocities in the Karakoram region from ALOS-1 PALSAR-1 summer FBD data and winter FBS images between 2007 and 2010.

18: ITS_LIVE provides low-delay measurements of glacier and ice sheet surface velocity from 1985 to present across the globe. These data are currently based on Landsat 5, 7, 8 and 9, Sentinel-2 and Sentinel-1 images. Data with a spatial resolution of 240 m can be downloaded and explored from NASA's Jet Propulsion Laboratory, California Institute of Technology website.

4. Climate data

4.1 Overview

Climate data are available from climate stations (point data at a certain elevation) or so-called reanalysis datasets (raster data of global scale) that are derived from back-calculating atmospheric conditions (for several elevations or pressure levels) by assimilating observations on the ground (climate stations) and in the air (radiosondes, airplanes) using weather forecast models. In this way, gaps in climate station coverage are filled by interpolation using physical principles (e.g. atmospheric motion). Due to different methods and models being applied as well as the rapid development in available computer power, reanalysis datasets are constantly improved (e.g. in spatial and temporal resolution). European reanalysis datasets evolved from ERA-40 to ERA-Interim to ERA5 Land. The latter provides a wide range of variables every hour since 1950 at about 9 km spatial resolution. These datasets might be aggregated to daily means and will be used to force the mass balance model and analyse climatic trends.

For practical purposes, the variables of interest have been extracted from these datasets and were aggregated over longer time periods, e.g. as seasonal, annual or multi-annual mean values over a given period of time. Of particular interest for this project are the related precipitation climatologies, which provide mean values of total precipitation over a given region. Most of these datasets have already been evaluated in the literature (e.g. Dahri et al. 2016, Liu and Margulis 2019) and we will come back to the related results when selecting specific ones for our applications (in the mass balance model for the Karakoram and the lager trends in HMA).

Table 2: Climate-related datasets and their sources. The URL for all datasets is listed below the table. P clim: precipitation climatology.

ID	Type	Name	Region	Epoch	Description	Reference	URL
C1	P clim.	TRMM 3b43	global	1998-present	Monthly precip at 0.25° from EO & station data	Huffman et al. 2007	1
C2	P clim.	WFDEI	global	1979-present	Combines ERA-Interrim (C4) with CRU & GPCC	Wedon et al. 2014	2
C3	Reanalysis	HAR2	HMA	1980-2023	See Section 4.2	Maussion et al. 2014, Wang et al. 2020	3
C4	Reanalysis	ERA Interrim	global	1979- 2019	See Section 4.2	Dee et al. 2011	4
C5a	Reanalysis	ERA 5	global	1950 - present	See Section 4.2, 31 km res., hourly	Hersbach et al. 2020	5
C5b	Reanalysis	ERA 5 Land	global	1950 - present	See Section 4.2, 9 km res., hourly	Munoz-Sabater et al. 2021	6
C6	Reanalysis	MERRA-2	global	from 1980	See Section 4.2	Gelaro et al. 2017	7
C7	Reanalysis	JRA-55	global	from 1958	See Section 4.2	Kobayashi et al. 2015	8
C8	Station T, P	Meteo data	Pakistan	1954 (1995) - present	From PMD & WAPDA	cited in many stusies	9
C9	Station	Urdukas & K2 Base Camp	Baltoro	since 2004, interuptions	At 4022 and 5033 m operated by EVK2CNR	via colleagues from Milan	10
C10	Cloud properties (e.g. cloud cover)	AVHRR-PMv3	global	1982-2016 (2020)	See Section 4.2	Stengel et al. (2020)	11
C11	Cloud properties (e.g. cloud dover)	SLSTR	global	2017-2024	Currently developed for C3S; avail. in July 2025	TBD	12

Dataset URL:
1: several sources
2: ftp site, to be checked
3: https://www.tu.berlin/en/klima/research/regional-climatology/high-asia/har
4: 3/6-hourly data: https://rda.ucar.edu/datasets/d627000/,
monthly: http://rda.ucar.edu/datasets/ds627.1/
5: https://cds.climate.copernicus.eu/datasets?q=ERA5
6: https://cds.climate.copernicus.eu/datasets?q=ERA5
7: Description, access links: https://gmao.gsfc.nasa.gov/reanalysis/MERRA-2/data_access/
8: 3/6-hourly data: https://rda.ucar.edu/datasets/d628000/,
monthly: https://rda.ucar.edu/datasets/d628001/
9: pmd.gov.pk, wapda.gov.pk
10: https://geoportal.mountaingenius.org/portal
11: https://doi.org/10.5676/DWD/ESA_Cloud_cci/AVHRR-PM/V003
12: TBD

4.2 Short descriptions

Below, we provide some further details to the datasets presented in Table 2 (sorted by ID).
C3: The High Asia Refined Analysis version 2 (HAR v2), TU Berlin at 10 km resolution. Compared to the old version, HAR v2 has a higher resolution, an extended domain and longer temporal coverage. Generated by dynamical downscaling using WRF, forced by ERA5 data and using snow depths from JRA-55 (since ERA5 overestimates snow depth over the Tibetan Plateau, Orsolini et al. 2019).

C4: ECMWF reanalysis available at sub-daily, daily and monthly intervals and at spatial resolution of 0.75° (about 79 km) now replaced by ERA5. Assimilates snow cover from the IMS product at 24 km resolution since 2004 and has been found to provide more realistic precipitation/snow values over the TP than ERA5 (Orsolini et al., 2019), but did not represent decadal precipitation trends that could explain lake level changes (Treichler et al. 2019).

C5a/b: Most recent version of ECMWF's reanalysis, produced by C3S. ERA5-Land is a dynamically downscaled version at higher resolution (ca. 9 km) than ERA 5 (31 km) but the latter has 131 elevation levels whereas ERA5-land only refers to the surface. Generally found to overestimate precipitation in many parts of HMA, but to underestimate high-altitude precipitation (Liu and Margulis 2019). According to Orsolini et al. (2019): "Unlike ERA-I, IMS data are not used above 1500 m, i.e. in high altitude regions, which includes the TP. No station data over the TP are used. Unlike ERA-I, the snow depth analysis is not relaxed toward a climatology when observations are unavailable."

C6: NASA Modern-Era Retrospective analysis for Research and Applications, Version 2 (MERRA-2). Performs an online correction for precipitation using data from the NOAA Climate Prediction Center (Unified Gauge-Based Analysis of Global Daily Precipitation CPCU, Merged Analysis of Precipitation CMAP). Found to represent more realistic snow volumes (Orsolini et al. 2019), high-altitude precipitation (Liu and Margulis 2019) and precipitation patterns that fit lake level changes (Treichler et al., 2019) compared to other reanalyses.

C7: The Japanese reanalysis JRA-55 includes an interpolation-based snow depth analysis and incorporates snow satellite information (SSM/I, SSMIS) and in situ observations of snow depth over the TP. It showed improved performance in representing snow cover/volumes (Orsolini et al. 2019).

C11: The Cloud_cci AVHRR-PMv3 dataset (covering 1982-2016, unofficial extension until 2020) was generated within the Cloud_cci project. This dataset is based on AVHRR (onboard NOAA-7, NOAA-9, NOAA-11, NOAA-14, NOAA-16, NOAA-18, NOAA-19) measurements and contains a variety of cloud properties which were derived employing the Community Cloud retrieval for Climate (CC4CL; Sus et al., 2018; McGarragh et al., 2018) retrieval framework. The core cloud properties contained in the Cloud_cci AVHRR-PMv3 dataset are cloud mask/fraction, cloud phase, cloud top pressure/height/temperature, cloud optical thickness, cloud effective radius and cloud liquid/ice water path. Spectral cloud albedo is also included as experimental product. The cloud properties are available at different processing levels: Level-3U (globally gridded, unaveraged data fields at 0.05°) and Level-3C (monthly averages and histograms at 0.5°). Pixel-based uncertainty estimates come along with all properties and are also propagated into Level-3C data. More details on the dataset can be found in Stengel et al. (2020).

C12: Dataset will be a successor of the CCI SLSTR cloud data currently available through C3S (https://cds.climate.copernicus.eu/datasets/satellite-cloud-properties?tab=overview) with higher spatial resolution, though, covering a short period.

5. Auxiliary data

5.1 Overview

The two main auxiliary datasets to be used for the project are a digital elevation model (DEM) and information about lake levels and extent, both listed in Table 4. Whereas DEM coverage will be restricted to the Karakoram perimeter, lake data will primarily be analysed outside the Karakoram, i.e. the Tibetan Plateau where most lakes are endorheic. For the DEM we will use already compiled datasets as is, lake data stem from various projects, mostly using optical sensors (Landsat, Sentinel-2) for extent and a range of altimetry sensors for lake level. Spatial altimetry allows the measurement of water level in rivers, lakes and floodplains. Since the early 1990s, several altimetry satellites have been launched, as shown in Fig. 5.1.

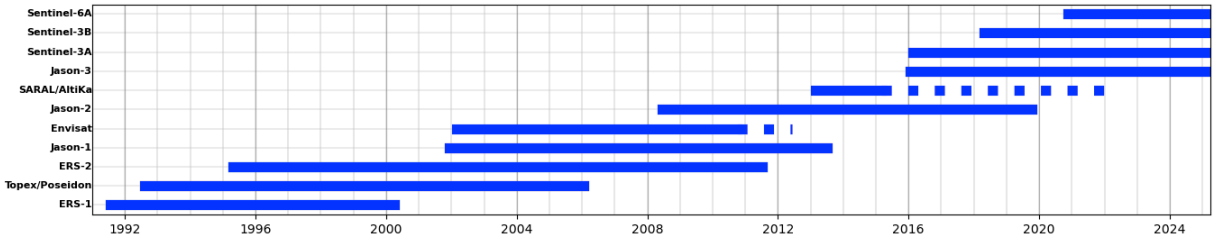

Fig. 5.1: Timeline for satellite altimeters. Dashed lines correspond to major orbit changes.

Their main objective is to measure ocean height, but their altimetry measurements can also be used to measure continental water levels (inland seas, rivers, lakes, flooded areas, reservoirs). The products are an important complement or even an alternative to in situ measurements, especially in regions where ground-based networks are either non-existent or degrading. Used in conjunction with other hydrological data and hydrological model outputs, these data make a valuable contribution to the study of the water cycle and the quantification of water resources. Due to their launch date, lifetime and orbit, a virtual station on a lake has been provided with partial or full coverage since 1992. The main altimetry satellites, their operation time and repeat period are provided in Table 3.

Table 3: Characteristics of main altimetry satellites.

Nr.	Satellite	Operation	Repeat Period (d)
1	Topex/Poseidon	1992-2002	10
	Jason-1	2002-2008	10
	Jason-2/OSTM	2008-2016	10
	Jason-3	2016-current	10
	Sentinel-6A MF	2020-current	10
	Sentinel-3A	2016-current	27
	Sentinel-3B	2018-current	27
	ERS-1	1992-1993, 1995-1996	35
	ERS-2	1996-2003	35
	ENVISAT	2002-2010	35
	SARAL	2013-2016	35

Table 4: Auxiliary datasets to be used in the project. The URL for all datasets is listed below the table.

ID	Type	Name	Region	Epoch	Description	Reference	URL
D1	DEM	Copernicus DEM GLO-30	Global	12/2010-01/2015	Global Digital Surface Model with 1'' pixel spacing referring to the EGM2008	see URL	1
D2	DEM	SRTM DEM	Global	Feb. 2000	Near global (60° N – 57° S) DEM at 1" resolution	see URL	2
L1	Lake extent	Lake_cci LWE	Global	varies	see Section 5.2	Lake_cci	3
L2	Lake level	Lake_cci LWL	Global	varies	see Section 5.2	Lake_cci	4
L3	Lake level / volume	HydroWEB.next	Global	varies	see Section 5.2	Crétaux et et al. 2011	5
L4	Lake level	C3S Lakes	Global	1992- now	see Section 5.2	C3S Lakes	6
L5	Lake level	DAHITI	Global	varies	see Section 5.2	Schwatke et al. 2015	7
L6	Lake level	G-REALM	Global	varies	see Section 5.2	Birkett & Beckley 2010	8
L7	Lake level / extent / volume	TPlakes	TP	1990-2015	see Section 5.2	Treichler et al. 2019	9
L8	Lake extent	Global Surface Water Explorer	Global	1984-2021	see Section 5.2	Pekel et al. 2016	10
L9	Lake extent	TPlakes	TP	1920-2020	see Section 5.2	Zhang et al. 2021	11

Dataset URL:
D1: https://doi.org/10.5270/ESA-c5d3d65 (dataspace.copernicus.eu)
D2: earthdata.nasa.gov, also void filled 90 m version 4.1 from CGIAR (various sources)
L1: https://climate.esa.int/en/projects/lakes/key-documents-lakes/
L3: https://hydroweb.next.theia-land.fr/
L4: Data / description: 10.24381/cds.5714c668
L5: https://dahiti.dgfi.tum.de/en/
L6: https://ipad.fas.usda.gov/cropexplorer/global_reservoir/
L7: dataset: 10.5281/zenodo.15015078
L8: https://global-surface-water.appspot.com/map
L9: dataset: https://doi.org/10.5281/zenodo.4678104

5.2 Short descriptions

Below, we provide some further details to the datasets presented in Table 4 (sorted by ID).

L1/L2: The ESA Lakes_cci project aims at gathering a compact dataset of water height and extent (among other ECVs) on 2024 lakes spread worldwide. The Lake Water Level (LWL) is estimated from altimetry measurement, and the Lake Water Extent (LWE) is derived from a hypsometric curve established from both altimetry and Sentinel-2 data (more info on the ATBD: https://climate.esa.int/en/projects/lakes/key-documents-lakes/). Other alternatives may provide LWL data if a lake of interest is not covered:

L3, HydroWEB.next: With the HydroWEB.next service (https://hydroweb.next.theia-land.fr/ – Crétaux et al., 2011) hosted on the platform of the national French THEIA cluster and operated by CLS, LEGOS-CNES has been developing, since 2003, a database of water level variations on lakes and rivers around the world based on satellite altimetry. As of March 2023, 12,546 virtual stations are monitored on rivers and 442 on lakes, all available in HydroWEB, in operational mode (real-time update) or in delayed mode. In addition, changes in extent and

volume are also measured for some of them. These observations allow the construction of long time series of water levels over continental surface waters.This database includes the Lakes_CCI water level time series. (Ref: Crétaux et al., 2011)

L4, C3S Lakes: In the frame of the C3S Lakes (Copernicus Climate Change Service), virtual stations on lakes are provided by CLS. They encompass the 311 lakes available on Hydroweb, but also more than 8,000 virtual stations on small lakes (more info on https://cds.climate.copernicus.eu/datasets/satellite-lake-water-level,
Ref: https://doi.org/10.24381/cds.5714c668).

L5, DAHITI: The Database for Hydrological Time Series of Inland Waters (DAHITI) was developed by the Deutsches Geodätisches Forschungsinstitut der Technischen Universität München (DGFI-TUM) in 2013 to provide water level time series of inland waters. Today, DAHITI develops a variety of hydrological information on lakes, reservoirs, rivers, and wetlands derived from satellite data, i.e., from multi-mission satellite altimetry and optical remote sensing imagery. As for Hydroweb, all products are available free of charge for the user community after a short registration process. As of March 2023, DAHITI currently provides 10 103 water level time series distributed over all continents, except Antarctica. In Africa (2082 time series), Asia (1737), Australia (46), Europe (680), North America (1395), and South America (4024) water level time series are available. 8,637 of these virtual stations follow rivers, 1,058 lakes and 387 reservoirs (Ref: Schwatke et al. 2015).

L6, G-REALM: The U.S. Department of Agriculture's Foreign Agricultural Service (USDA-FAS), in co-operation with the National Aeronautics and Space Administration, and the University of Maryland, are routinely monitoring lake and reservoir height variations for many large lakes around the world. This program is called Global Reservoir and Lake Monitoring (G-REALM) (Birkett & Beckley 2010). It utilizes NASA/CNES/ESA/ISRO radar altimeter data over inland water bodies in an operational manner. The surface elevation products are produced via a semi-automated process and placed on the G-REALM website for USDA and public viewing. As of November 2022, 530 lakes are monitored, and their water height time series can be viewed and downloaded at ipad.fas.usda.gov/cropexplorer/global_reservoir.

L7: Lake extent time series for endorheic lakes on the TP (1347 lakes) extracted from Landsat imagery, lake level elevations from SRTM DEM elevations of the lake shoreline for each year (1009 lakes), and ICESat laser altimetry measurements of the lake surface (103 lakes), extended beyond the 2003-2009 ICESat measurement period by applying the area–surface-elevation relationship for each lake to measured lake areas for earlier/later years. Annual water volume changes from multiplying annual lake areas and water level changes.

L8: Location and temporal distribution of water surfaces at the global scale over the past 3.8 decades, statistics on the extent and change of those water surfaces. Produced from Landsat imagery, interactive map explorer.

L9: Lake evolution on the TP from 1920 to 2020 (Chinese part only) and over the entire TP area above 2500 m asl for 1970 to 2020. The lake mapping in 1920 is derived from early Chinese map data, in 1960 from the topographic map by manual digitizing, and from 1970 to 2020 derived from Landsat MSS, TM, ETM+ and OLI images by semi-automatic water classification.

References

Glacier data

Berthier, E. and Brun, F. (2019). Karakoram geodetic glacier mass balances between 2008 and 2016: persistence of the anomaly and influence of a large rock avalanche on Siachen Glacier. Journal of Glaciology, 65 (251), 494-507.

Bhambri, R., Hewitt, K., Kawishwar, P., & Pratap, B. (2017). Surge-type and surge-modified glaciers in the Karakoram. Scientific Reports, 7(1), doi.org/10.1038/s41598-017-15473-8.

Dahri, Z. H., Ludwig, F., Moors, E., Ahmad, B., Khan, A. and Kabat, P. (2016). An appraisal of precipitation distribution in the high-altitude catchments of the Indus basin. Science of the Total Environment, 548, 289-306.

Dehecq, A., Gourmelen, N., Gardner, A. S., Brun, F., Goldberg, D., Nienow, P. W., Berthier, E., Vincent, C., Wagnon, P. & Trouvé, E. (2019). Twenty-first century glacier slowdown driven by mass loss in High Mountain Asia. Nature Geoscience, 12(1), 22-27.

Gardner, A. S., M. A. Fahnestock, and T. A. Scambos (2019a). ITS_LIVE Regional Glacier and Ice Sheet Surface Velocities: Version 1. Data archived at National Snow and Ice Data Center; https://doi:10.5067/6II6VW8LLWJ7

Gardner, A. S., M. A. Fahnestock, and T. A. Scambos (2019b). MEaSUREs ITS_LIVE Landsat Image-Pair Glacier and Ice Sheet Surface Velocities: Version 1. Data archived at National Snow and Ice Data Center. https://doi.org/10.5067/IMR9D3PEI28U

Herreid, S. and Pellicciotti, F. (2020). The state of rock debris covering Earth's glaciers. Nature Geoscience, 13 (9), 621-627.

Hugonnet, R., McNabb, R., Berthier, E., Menounos, B., Nuth, C., Girod, L., Farinotti, D., Huss, M., Dussaillant, I., Brun, F. and Kaeaeb, A. (2021). Accelerated global glacier mass loss in the early twenty-first century. Nature, 592, 726-731.

Mayer, C., Lambrecht, A., Oerter, H., Schwikowski, M., Vuillermoz, E., Frank, N. and Diolaiuti, G. (2014). Accumulation studies at a high elevation glacier site in central Karakoram. Advances in Meteorology, Article ID 215162; doi.org/10.1155/2014/215162

Mihalcea, C., Mayer, C., Diolaiuti, G., D'Agata, C., Smiraglia, C., Lambrecht, A., Vuillermoz, E. and Tartari, G. (2008). Spatial distribution of debris thickness and melting from remote-sensing and meteorological data, at debris-covered Baltoro glacier, Karakoram, Pakistan. Annals of Glaciology, 48, 49-57.

Millan, R., J. Mouginot, A. Rabatel, and M. Morlighem (2022). Ice velocity and thickness of the world's glaciers. Nature Geoscience, 15 (2), 124–129.

Muñoz-Sabater, J., Dutra, E., Agustí-Panareda, A., Albergel, C., Arduini, G., Balsamo, G., Boussetta, S., Choulga, M., Harrigan, S., Hersbach, H., Martens, B., Miralles, D. G., Piles, M., Rodríguez-Fernández, N. J., Zsoter, E., Buontempo, C., and Thépaut, J.-N. (2021). ERA5-Land: a state-of-the-art global reanalysis dataset for land applications. Earth Syst. Sci. Data, 13, 4349–4383, doi.org/10.5194/essd-13-4349-2021

Paul, F., T. Bolch, A. Kääb, T. Nagler, C. Nuth, K. Scharrer, A. Shepherd, T. Strozzi, F. Ticconi, R. Bhambri, E. Berthier, S. Bevan, N. Gourmelen, T. Heid, S. Jeong, M. Kunz, T.R. Lauknes, A. Luckman, J. Merryman, G. Moholdt, A. Muir, J. Neelmeijer, M. Rankl, J. Van Looy and T. Van Niel (2015). The glaciers climate change initiative: Methods for creating glacier area, elevation change and velocity products, Remote Sensing of Environment, 162: 408–426, doi: 10.1016/j.rse.2013.07.043

Racoviteanu, A.E., Rittger, K. and Armstrong, R. (2019). An Automated Approach for Estimating Snowline Altitudes in the Karakoram and Eastern Himalaya From Remote Sensing. Front. Earth Sci., 7, 220; doi.org/10.3389/feart.2019.00220

Rankl, M., Kienholz, C. and Braun, M. (2014). Glacier changes in the Karakoram region mapped by multimission satellite imagery. The Cryosphere, 8(3), 977-989.

Rounce, D. R., Hock, R., McNabb, R. W., Millan, R., Sommer, C., Braun, M. H., et al. (2021). Distributed global debris thickness estimates reveal debris significantly impacts glacier mass balance. Geophysical Research Letters, 48, e2020GL091311. https://doi.org/10.1029/2020GL091311

Scherler, D., Wulf, H. and Gorelick, N. (2018). Global assessment of supraglacial debris-cover extents. Geophysical Research Letters, 45. 11798-11805.

Shean, D.E., Bhushan, S., Montesano, P., Rounce, D.R., Arendt, A. and Osmanoglu, B. (2020). A systematic, regional assessment of high mountain Asia glacier mass balance. Frontiers in Earth Science, 7, 363; doi.org/10.3389/feart.2019.00363.

Climate data:

Dee, D. P., Uppala, S. M., Simmons, A. J., Berrisford, P., Poli, P., Kobayashi, S., Andrae U., Balmaseda, M. A., Balsamo, G., Bauer, P. Bechtold, P., Beljaars, A. C. M., van de Berg, L., Bidlot, J., Bormann, N., Delsol, C., Dragani, R., Fuentes, M., Geer, A. J., Haimberger, L., Healy, S. B., Hersbach, H., Hólm, E. V., Isaksen, L., Kållberg, P., Köhler, M., Matricardi, M., McNally, A. P., Monge-Sanz, B. M., Morcrette, J.-J., Park, B.-K., Peubey, C., de Rosnay, P.,Tavolato, C., Thépaut, J.-N., and Vitart, F. (2011). The ERA-Interim reanalysis: configuration and performance of the data assimilation system, Q. J. Roy. Meteor. Soc., 137, 553–597.

Gelaro, R., McCarty, W., Suárez, M. J., Todlinga, R., Moloda, A., Takacs, L., Randles, C. A., Darmenov, A., Bosilovich, M. G., Reichle, R., Wargan, K., Coy, L., Cullather, R., Draper, C., Akella, S., Buchard, V., Conaty, A., da Silva, A. M., Gu, W., Kim, G.-K., Koster, R., Lucchesi, R., Merkova, D., Nielsen, J. E., Partyka, G., Pawson, S., Putman, W., Rienecker, M., Schubert, S. D., Sienkiewicz, M., and Zhao, B.: The Modern-Era Retrospective Analysis for Research and Applications, Version 2 (MERRA-2), J. Climate, 30, 5419–5454, 2017.

Hersbach H, Bell B, Berrisford P, et al. The ERA5 global reanalysis. Q J R Meteorol Soc. 2020; 146: 1999–2049. https://doi.org/10.1002/qj.3803

Huffman, G.J., Adler, R.F., Bolvin, D.T., Gu, G., Nelkin, E.J., Bowman, K.P., Hong, Y., Stocker, E.F. and Wolff, D.B. (2007). The TRMM Multisatellite Precipitation Analysis (TMPA): quasiglobal, multiyear, combined-sensor precipitation estimates at fine scales. J. Hydrometeorol. 8, 38–55. http://doi.org/10.1175/JHM560.1

Kobayashi, S., Ota, Y., Harada, Y., Ebita, A., Moriya, M., Onoda, H., Onogi, K., Kamahori, H., Kobayashi, C., Endo, H., Miyaoka, K., and Takahashi, K. (2015) The JRA-55 Reanalysis: General specifications and basic characteristics. J. Meteorol. Soc. Jpn., 93, 5–48, https://doi.org/10.2151/jmsj.2015-001

Liu, Y. and Margulis, S.A. (2019). Deriving Bias and Uncertainty in MERRA-2 Snowfall Precipitation Over High Mountain Asia. Front. Earth Sci., 7, 280. doi.org/10.3389/feart.2019.00280

Maussion, F., Scherer, D., Mölg, T., Collier, E., Curio, J. and Finkelnburg, R. (2014). Precipitation seasonality and variability over the Tibetan Plateau as resolved by the High Asia Reanalysis. Journal of Climate, 27 (5), 1910-1927.

McGarragh et al. (2018): The Community Cloud retrieval for CLimate (CC4CL) Part 2: The optimal estimation approach, Atmos. Meas. Tech., 11, 3397-3431, doi.org/10.5194/amt-11-3397-2018

Orsolini, Y., Wegmann, M., Dutra, E., Liu, B., Balsamo, G., Yang, K., de Rosnay, P., Zhu, C., Wang, W., Senan, R., and Arduini, G. (2019). Evaluation of snow depth and snow cover over the Tibetan Plateau in global reanalyses using in situ and satellite remote sensing observations. The Cryosphere, 13, 2221–2239, https://doi.org/10.5194/tc-13-2221-2019

Sus et al. (2018). The Community Cloud retrieval for CLimate (CC4CL) Part 1: A framework applied to multiple satellite imaging sensors, Atmos. Meas. Tech., 11, 3373-3396, https://doi.org/10.5194/amt-11-3373-2018, 2018

Stengel et al. (2020). Cloud_cci Advanced Very High Resolution Radiometer post meridiem (AVHRR-PM) dataset version 3: 35-year climatology of global cloud and radiation properties. Earth Syst. Sci. Data, 12, 4160, https://doi.org/10.5194/essd-12-41-2020, 2020.

Wang, X., Tolksdorf, V., Otto, M., Scherer, D. (2020). WRF–based dynamical downscaling of ERA5 reanalysis data for High Mountain Asia: Towards a new version of the High Asia Refined analysis. International Journal of Climatology, 41, 743–762.

Auxiliary data

Birkett, C. M., & Beckley, B. (2010). Investigating the Performance of the Jason-2/OSTM Radar Altimeter over Lakes and Reservoirs. Marine Geodesy, 33(sup1), 204-238. https://doi.org/10.1080/01490419.2010.488983

Crétaux, J.-F., Arsen, A., Calmant, S., Kouraev, A., Vuglinski, V., Bergé-Nguyen, M., Gennero, M.-C., Nino, F., Abarca Del Rio, R., Cazenave, A., & Maisongrande, P. (2011). SOLS : A lake database to monitor in the Near Real Time water level and storage variations from remote sensing data. Advances in Space Research, 47(9), 1497-1507. https://doi.org/10.1016/j.asr.2011.01.004

Pekel, J.-F., Cottam, A., Gorelick, N. and Belward, A.S. (2016). High-resolution mapping of global surface water and its long-term changes, Nature, 540, 418–422; doi.org/10.1038/nature20584.

Schwaizer, G., Nagler, T., Hetzenecker, M., Mölg, N., Metsämäki, S., and Nemec, J. (2024): ESA Snow Climate Change Initiative (Snow_cci): Daily global Snow Cover Fraction - snow on ground (SCFG) from MODIS (2000-2022), version 3.0. NERC EDS Centre for Environmental Data Analysis, 15.10.2024; doi.org/10.5285/80567d38de3f4b038ee6e6e53ed1af8a

Schwatke, C., Dettmering, D., Bosch, W., & Seitz, F. (2015). DAHITI – an innovative approach for estimating water level time series over inland waters using multi-mission satellite altimetry. Hydrology and Earth System Sciences, 19(10), 4345-4364. https://doi.org/10.5194/hess-19-4345-2015

Treichler, D., Kääb, A., Salzmann, N., and Xu, C.-Y.: Recent glacier and lake changes in High Mountain Asia and their relation to precipitation changes, The Cryosphere, 13, 2977–3005, https://doi.org/10.5194/tc-13-2977-2019, 2019.

Zhang, G., Ran, Y., Wan, W., Luo, W., Chen, W., Xu, F., and Li, X.: 100 years of lake evolution over the Qinghai–Tibet Plateau, Earth Syst. Sci. Data, 13, 3951–3966, https://doi.org/10.5194/essd-13-3951-2021, 2021.

Acronyms

AAR	Accumulation Area Ratio
a.s.l.	above sea level
ASTER	Advanced Spaceborne Thermal Emission and Reflection radiometer
CKNP	Central Karakoram National Park
ELA	Equilibrium Line Altitude
ERA	European Reanalysis
DEM	Digital Elevation Model
GLOF	Glacier Lake Outburst Flood
GloGEM	Global Glacier Evolution Model
HMA	High Mountain Asia
ICESat	Ice, Cloud, and land Elevation Satellite
IPCC	Intergovernmental Panel on Climate Change
NASA	National Aeronautics and Space Administration
MODIS	Moderate Resolution Imaging Spectrometer
PDD	Positive Degree Day
SAR	Synthetic Aperture Radar
SMB	Surface Mass Balance
SNR	Signal to Noise Ratio
SRTM	Shuttle Radar Topography Mission
UIB	Upper Indus Basin
w.e.	water equivalent
WGMS	World Glacier Monitoring Service